JOURNAL OF MATERIALS SCIENCE **35** (2000) 375–380

Solidification mode and residual ferrite in low-Ni austenitic stainless steels

A. DI SCHINO
Materials Engineering Centre, University of Perugia, Terni, Italy

M. G. MECOZZI, M. BARTERI
Centro Sviluppo Materiali, Italy

J. M. KENNY
Materials Engineering Centre, University of Perugia, Terni, Italy
E-mail: kenny@unipg.it

The solidification modes of two new classes of austenitic stainless steels with a low content of Ni are shown. Their chemical composition is similar to that of the standard AISI 304 and AISI 316, except for the content of nickel, manganese and nitrogen. It is found that standard formulas for predicting the residual ferrite can be fairly well used in the prediction of the solidification mode while they do not work in predicting the residual ferrite content. In particular, it is found that ferrite is the first phase to solidify for values of the equivalent ratio (calculated according to the formulas developed by Hammar and Svensson) greater than 1.50, otherwise austenite is the first phase to solidify. A new set of equations for predicting the residual δ-ferrite in these new classes of materials is determined via multivariable linear regression. The influence of the steel solidification mode on the material structural transformations during heat treatment is also shown.

1. Introduction

Nickel, Ni-alloys and, in particular, nickel containing austenitic stainless steels have been indispensable for the progress of technology during the past 80 years. Our modern technology and high standard of life would not have been achieved without nickel containing alloys. Due to the high cost of nickel and to the increasing attention to nickel allergic reactions, more and more laboratories and industries are trying to develop a new class of austenitic stainless steels with a low content of nickel and with mechanical and corrosion properties comparable to those of standard nickel based materials [1]. In the development of a new austenitic stainless steel, modifying the chemical composition of a standard one, a detailed knowledge of the effect of this change on the solidification mode and ferrite content is necessary.

Metallurgists have been very active in developing basic scientific research on solidification of various metallic materials. In particular, in the field of stainless steels, as steel makers move to the continuous casting of increasingly highly alloyed steels, it becomes more and more important to determine the solidification modes, since these determine the castability, the hot workability and the room temperature structure.

Four mechanisms or modes explain the stainless steels solidification, namely:

mode A: $\mathrm{L} \rightarrow \mathrm{L} + \delta \rightarrow \delta \rightarrow \delta + \gamma$

mode B: $\mathrm{L} \rightarrow \mathrm{L} + \delta \rightarrow \mathrm{L} + \delta + \gamma \rightarrow \delta + \gamma \rightarrow \gamma$

mode C: $\mathrm{L} \rightarrow \mathrm{L} + \gamma \rightarrow \mathrm{L} + \gamma + \delta \rightarrow \gamma + \delta \rightarrow \gamma$

mode D: $\mathrm{L} \rightarrow \mathrm{L} + \gamma \rightarrow \gamma$

where L, δ and γ represent liquid, ferrite and austenite respectively.

These modes are illustrated schematically on a vertical section through the Fe-Ni-Cr phase diagram in Fig. 1. The solidification sequence and the subsequent transformation characteristics determine both the level of segregation and the distribution of the residual ferrite. Segregation is more deleterious in steels solidifying as primary austenite (mode D), since segregation at grain boundaries will not be redistributed by solid state transformations as it occurs with modes A, B and C [2]. Moreover the ferrite present in these last three modes may be dendritic or interdendritic depending on the solidification mode. The dendritic ferrite formed as a primary phase is not enriched in solute elements, unlike the interdendritic δ-ferrite, which forms as a result of segregation.

In this paper the solidification modes and the residual ferrite content of two new families of low-nickel austenitic stainless steels are examined. These new alloys are mainly characterised by a strong Ni reduction, which is compensated by manganese and nitrogen addition.

2. Literature equations for predicting solidification mode and residual ferrite

Complex austenitic stainless steel compositions can be reduced to simple Fe-Ni-Cr ternary alloys by the use of Cr and Ni equivalent compositions. Various sets of equations are available for predicting both the solidification modes and the residual ferrite content in

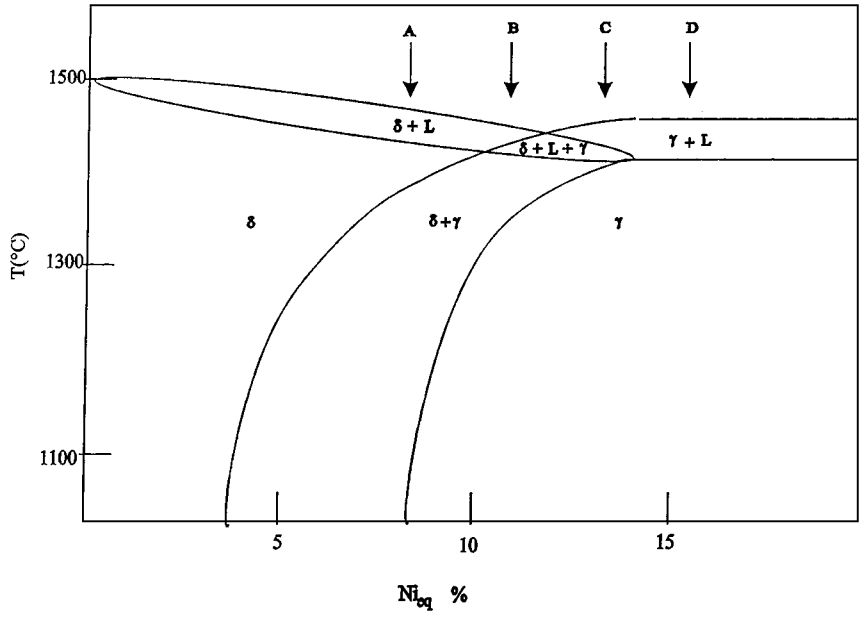

Figure 1 Section of the Fe-Ni-Cr phase diagram at 19% Cr showing solidification modes. $Ni_{eq} = (\%Ni) + 22(\%C) + 14.2(\%N) + 0.31(\%Mn) + (\%Cu)$.

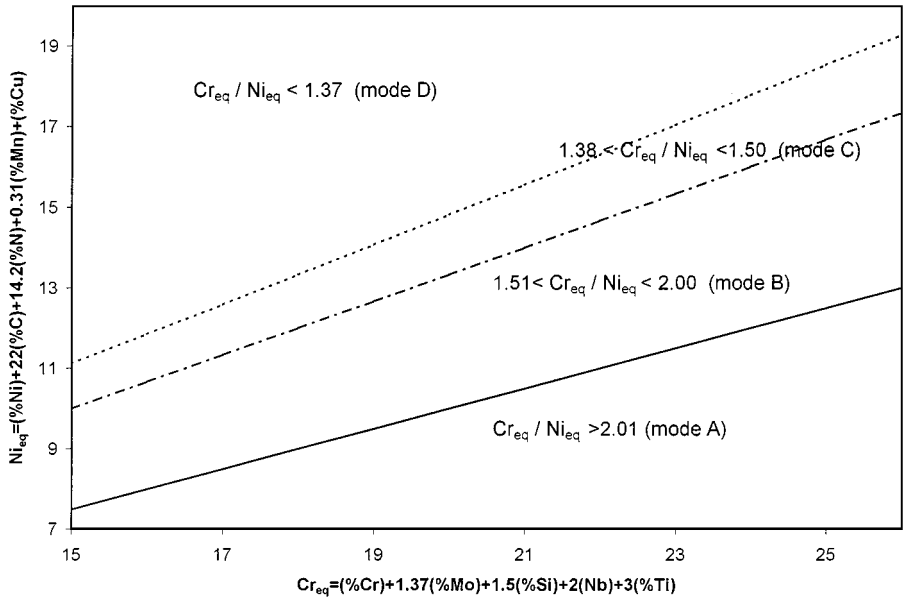

Figure 2 Solidification modes diagram for austenitic stainless steels.

austenitic stainless steels. One set of equations, which has proved to be successful in determining the solidification modes, has been proposed by Hammar and Svensson [3]:

$$Cr_{eq} = (\%Cr) + 1.37(\%Mo) + 1.5(\%Si) + 2(\%Nb) + 3(\%Ti) \quad (1)$$

$$Ni_{eq} = (\%Ni) + 22(\%C) + 14.2(\%N) + 0.31(\%Mn) + (\%Cu) \quad (2)$$

By using equivalent compositions, it is possible to apply the Fe-Cr-Ni phase diagram to predict the solidification sequence. A typical example is shown in Fig. 2. This approach has been very successful for the prediction of solidification modes in low alloyed stainless steels, where the value $Cr_{eq}/Ni_{eq} = 1.50$ can be used to define the boundary between primary ferritic and primary austenitic solidification modes of stainless steels.

Other equivalent compositions commonly used in the prediction of the solidification modes in low alloyed stainless steels are those reported by Jernkontoret [4], calculated according to equations very similar to (1) and (2). El Nayal and Beech [5] following the same approach found a good agreement between determined and predicted modes in solidifying low alloyed stainless steels. They found the following phase fields:

$$\frac{Cr_{eq}}{Ni_{eq}} < 1.37 \quad \text{(mode D)} \quad (3)$$

$$\frac{Cr_{eq}}{Ni_{eq}} = 1.38\text{–}1.70 \quad \text{(mode C)} \quad (4)$$

$$\frac{Cr_{eq}}{Ni_{eq}} = 1.71–2.00 \quad \text{(mode B)} \tag{5}$$

$$\frac{Cr_{eq}}{Ni_{eq}} > 2.01 \quad \text{(mode A)} \tag{6}$$

The main solid state phase transformation in austenitic stainless steels is the dissolution of ferrite, which can occur either isothermally or during cooling. The transformation seldom goes to completion and determines the presence of residual ferrite in the room temperature structure. Many methods have been developed for predicting the residual ferrite, which normally rely on the use of equations similar to those developed by De Long [6]:

$$\delta\% = 166.66(Cr_{eq}/Ni_{eq} - 0.738) \tag{7}$$

$$Cr_{eq} = (\%Cr) + (\%Mo) + 1.5(\%Si) + 2.5(\%Al + \%Ti) + 18 \tag{8}$$

$$Ni_{eq} = (\%Ni) + 30(\%C + \%N) + 0.5(\%Mn) + 36 \tag{9}$$

Although these formulas were developed for the prediction of ferrite content in the weld, they work fairly well in the prediction of solidification processes of standard austenitic stainless steels. Several modifications have been introduced in them for the prediction of residual ferrite in high nitrogen and manganese alloys. Hull [7] established that Mn acts as austenite-forming when used in low contents and as a ferritic element when used in high contents, in the presence of low contents of Ni and high contents of N.

3. Materials

Several ingots of low nickel austenitic steels have been produced. The austenite stability was guaranteed by adding nitrogen, which is well known as an austenite-forming element. A high content of Mn is required to attain the high nitrogen concentration in the melt [8]. The selected compositions, apart from these elements, were close to those of AISI 304 and AISI 316. The chemical composition of the 304-like steel ingots (called 304-LNi) lies in the range shown in Table I. The chemical composition of the 316-like steel ingots (called 316-LNi) lies in the range shown in Table II.

4. Results and discussion

4.1. Prediction of the solidification mode

A preliminary thermodynamical analysis was performed to predict the solidification modes of two different as cast ingots. The chemical composition of the ingots (namely number 244 and 248) is shown in Table III. Thermodynamic analysis by Thermocalc [9] predicts for both materials, under equilibrium conditions, a primary ferritic solidification mode as shown in the phase diagrams reported in Figs 3 and 4. The cooling line in the phase diagram corresponding to the chemical composition of alloy 248 (Fig. 3) is nearer

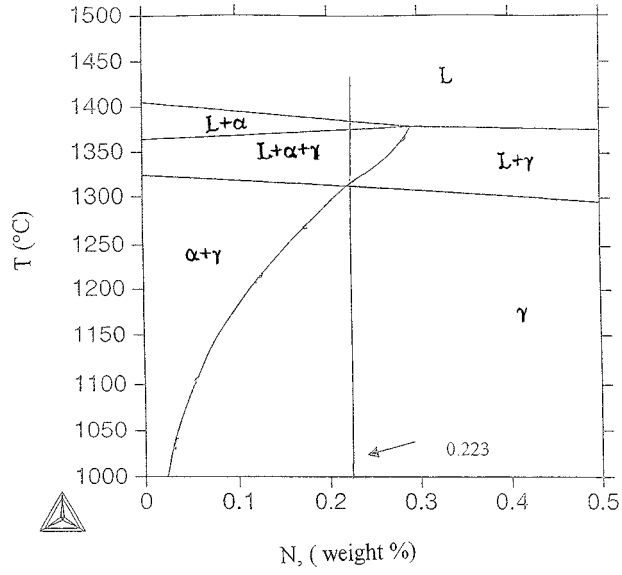

Figure 3 Thermodynamic analysis by Thermocalc for ingots 248.

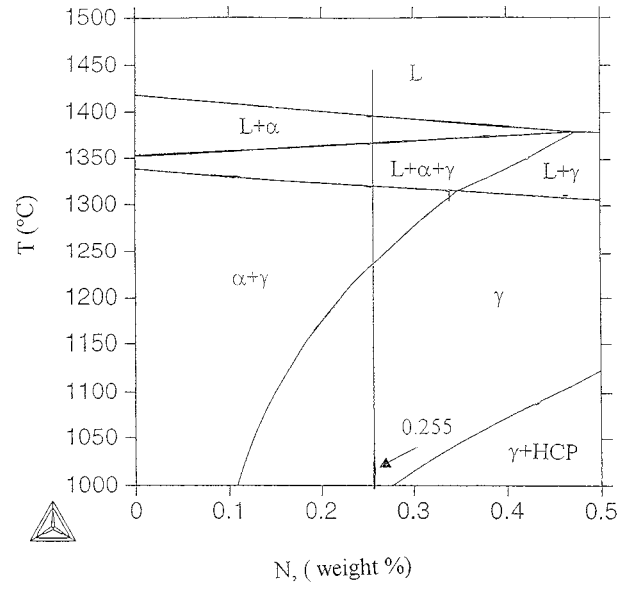

Figure 4 Thermodynamic analysis by Thermocalc for ingots 244.

to the primary austenitic solidification mode with respect to that of alloy 244 (Fig. 4). In non-equilibrium conditions, like those in the analysed solidification processes, a change in the solidification mode with respect to that predicted by the equilibrium phase diagrams is expected in the former alloy, depending on the test conditions (moderate to high cooling rates).

The microstructure of the two as cast ingots of 316-LNi was examined after etching with the Leicthnegger reagent. This etch makes yellow the Ni rich austenite and blue the Ni poor austenite, while ferrite remains white or, if the ferrite networks are particularly fine, black. The etch clearly distinguishes between primary dendrites and interdendritic spaces.

The morphology of ferrite and of austenite in ingots 244 and 248 is shown in Fig. 5. This morphology can be used to determine the first solidified phase and, hence, the solidification mode. The presence of interdendritic ferrite in alloy 248 (Fig. 5a and b) is indicative of modes C and D of solidification ($Cr_{eq}/Ni_{eq} < 1.50$).

TABLE I Chemical composition of 304 L-Ni ingots

	C	Si	Mn	Ni	Cu	Cr	N	Mo
Minimum	0.05	0.00	5.00	0.00	0.00	14.00	0.07	0.00
Maximum	0.12	1.00	13.00	2.00	3.00	20.00	0.50	1.00

TABLE II Chemical composition of 316 L-Ni ingots

	C	Si	Mn	Ni	Cu	Cr	N	Mo
Minimum	0.01	0.10	6.00	2.00	—	14.00	0.07	—
Maximum	0.13	2.00	14.00	7.00	4.00	20.00	0.50	3.00

TABLE III Chemical compositions of samples 244 and 248. The ratio Cr_{eq}/Ni_{eq} is calculated according to (1) and (2)

	C	Si	Mn	Ni	Cr	Mo	Cu	N	Cr_{eq}/Ni_{eq}
244	0.028	0.35	8.27	4.08	17.39	1.97	2.06	0.255	1.59
248	0.064	0.41	7.23	6.07	17.6	1.97	2.03	0.223	1.40

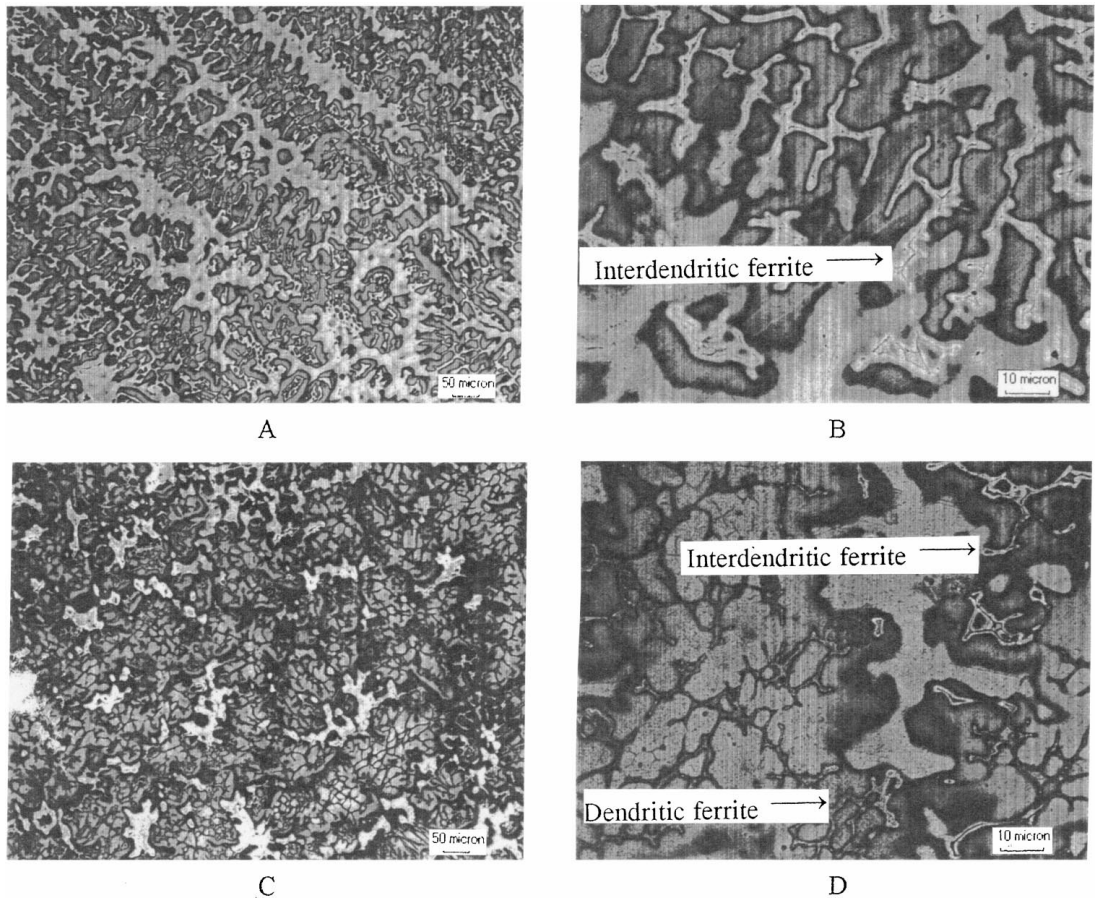

Figure 5 Optical micrographs of samples 248 (a and b) and 244 (c and d).

A particularly interesting structure is observed in the ingot 244 ($Cr_{eq}/Ni_{eq} = 1.59$), where regions of primary ferritic solidification coexist with regions of primary austenite (Fig. 5c and d). These results can be explained in terms of Equations 3–6 which predict primary ferritic solidification for values of the equivalents ratios (calculated accordingly Hammar and Svensson) greater than 1.50 (as in 244) and primary austenitic solidification for values lower than 1.50 (as in 248). That shows the formulas by Hammar and Svensson work fairly well for the prediction of solidification modes in spite of the high value of Mn and N contents.

Although Thermocalc results show that the equilibrium solidification structure should be ferritic for both materials analyzed, typical non-equilibrium conditions used in real solidification processes justify the austenitic structure obtained in the 248 ingot case.

4.2. Prediction of the residual ferrite content

For the prediction of the ferrite content, 77 buttons having different compositions within the 316-LNi range and 428 buttons over the 304-LNi range were produced.

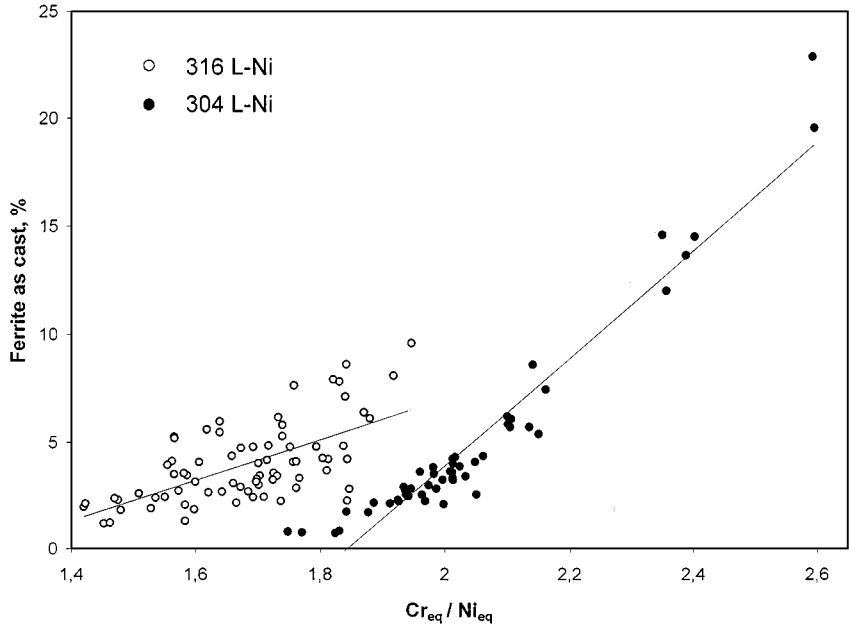

Figure 6 Ferrite content in the 316-LNi and in the 304 LNi as cast buttons. The ratio Cr_{eq}/Ni_{eq} is calculated according to equations 10–12 and 13–15 for the 316-LNi and the 304-LNi respectively.

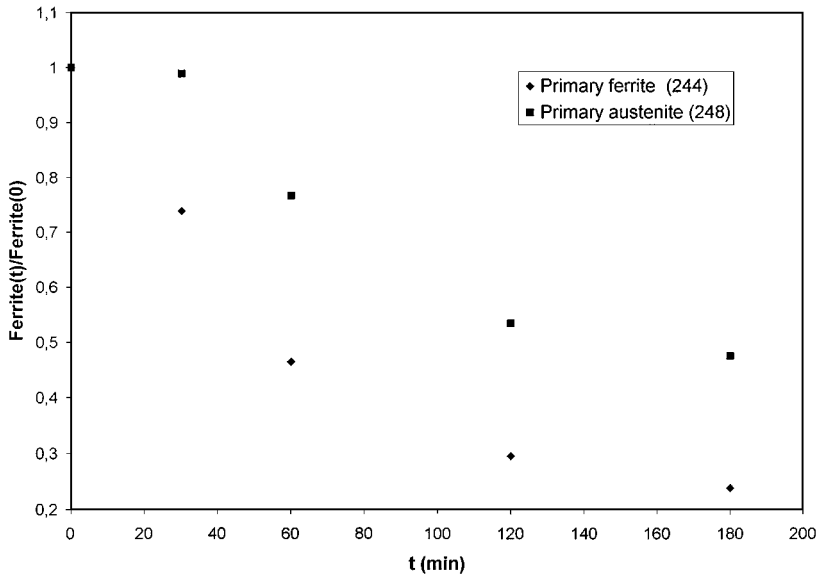

Figure 7 Influence of the solidification mode on the ferrite content on primary ferritic and primary austenitic solidifying steels during heat treatment. Ferrite(t) is the residual ferrite measured at time t, Ferrite(0) is the residual ferrite measured at time $t = 0$.

After chemical analysis, they were tested for residual ferrite content by a magnetic measuring. The given values are the average of 12 measure points per button on its sandpapered surface. The δ-ferrite content on both series of materials is not fitted by the De Long formulas (7)–(9). Therefore new Cr and Ni equivalents were assessed for the used composition range [10].

Typical components of the two families of steels (304-LNi and 316 LNi) are present in similar concentrations with the exception of Ni and Mo (see Tables I and II). As a consequence of this difference it is not possible to use the same equation for the prediction of ferrite content in both families. Then, two specific set of equations were developed. Thus, the composition/ferrite data of 316-LNi buttons were processed by multivariable linear regression to develop the following correlations:

$$\%\text{Ferrite} = 2.43(1.19\text{Cr}_{eq} - \text{Ni}_{eq} - 10.59) \quad (10)$$

$$\text{Cr}_{eq} = \text{Cr} + 0.55\text{Si} + 1.17\text{Mo} + 0.069\text{Mn} \quad (11)$$

$$\text{Ni}_{eq} = \text{Ni} + 25.17\text{C} + 21.68\text{N} + .21\text{Cu} \quad (12)$$

$$R^2 = 0.9126$$

On the other hand similar correlations were obtained for 304-LNi buttons:

$$\%\text{Ferrite} = 5.602(-10.66 + \text{Cr}_{eq} - \text{Ni}_{eq}/1.73) \quad (13)$$

$$\text{Cr}_{eq} = \text{Cr} + 0.62\text{Si} + 1.12\text{Mo} \quad (14)$$

$$\text{Ni}_{eq} = \text{Ni} + 36.4\text{C} + 27.5\text{N} + 0.54\text{Cu} + 0.01\text{Mn} + 0.01\text{Mn} \quad (15)$$

$$R^2 = 0.946$$

It is interesting to note that Mn acts as a ferritic element in formulas (10)–(12) developed for a high Mn steel. Moreover has just a small influence on the value of Ni_{eq} in formulas (13)–(15). Also this fact is in agreement with Hull [7]. However, the presence of a high content of Mn in this class of materials is required to favour the solubilisation of high levels of nitrogen [8]. The measured ferrite content in the two series of buttons is shown in Fig. 6 plotted versus Cr_{eq}/Ni_{eq} calculated according (10)–(12) and (13)–(15) for the 316-LNi and 304-LNi respectively.

The effect of the ferrite morphology is also evident in heating process (Fig. 7): ingots 244 and 248 were heated at 1200 °C for different times and then the ferrite content was measured by automatic imaging analysis. The sample having primary ferrite (244) shows a more rapid homogenisation of the structure.

Moreover, the dendritic ferrite will in most cases disappear more quickly than the interdendritic one during the cooling. These findings can be used to justify the observation that the surface regions of stainless steels ingots have a ferrite content lower than the one of the central regions. In fact, the cooling rate at the surface, faster that than at the centre, produces a finer dendrite arm spacing. The resultant fine structure is then more rapidly homogenised on cooling below the solidus line [4].

5. Conclusions

The solidification process of a new class of low-nickel austenitic stainless steels was examined. Although classical formulas cannot be applied to the class of materials examined here for the prediction of the residual ferrite, they work fairly well in the prediction of its solidification mode. In particular if the equivalent ratios calculated accordingly the classical formulas developed by Hammar and Svensson are greater than 1.50 the ferrite is the first phase to precipitate, otherwise austenite is the first phase to solidify. The influence of the steel solidification mode on the material structural transformations during the heat treatment has been also shown. In fact samples showing primary ferrite are more quickly homogenised than those showing primary austenite only.

Acknowledgements

Thanks are due to Acerinox and in particular to Dr. R. Sanchez for supplying test material and for the permission to use their ferrite measurements.

References

1. A. DI SCHINO, J. M. KENNY, M. G. MECOZZI and M. BARTERI, in Proceedings of the Sampe Internationale Conference, Paris, (1999), p. 175.
2. G. K. ALLAN, *Ironmaking and Steelmaking* **22** (1995) 465.
3. O. HAMMAR and U. SVENSSONN, "Solidification and Casting of Metals" (The Metal Society, London, 1997) p. 401.
4. JERNKONTORET, "A Guide to Solidification of Steels," edited by Jernkontoret (The Swedish Steel Producers Association, Stockolm, 1997).
5. G. EL NAYAL and J. BEECH, *Mat. Sci. Technol.* **2** (1986) 603.
6. C. J. LONG and W. T. DELONG, *Weld. J. Res. Suppl.* **52** (1973) 218.
7. F. C. HULL, *Weld. Journ.* **52** (1973) 193.
8. A. RECHSTEINER and M. O. SPEIDEL, in "Proceedings of the 1st European Stainless Steel Conference," edited by AIM, Florence 1997, Vol. 2, p. 107.
9. B. SUNDMAN, B. JANSSON and J. O. ANNDERSON, *Calphad* **9** (1985) 153.
10. M. BARTERI and F. FERNANDEZ de la MATA, *Acero inoxidable austenitico con niquel inferior al 2%*, EUR 16019 ES (1997).

Received 18 August 1998
and accepted 21 June 1999